Assembling gold nanoparticles in solution using phosphorothioate DNA as structural interconnects

Ashavani Kumar[†], Sumant Phadtare[†], Renu Pasricha[†], Piotr Guga[‡], Krishna N. Ganesh[*] and Murali Sastry[†,#]

[†]Materials Division and *Organic Chemistry (Synthesis) Division, National Chemical Laboratory, Pune 411 008, India
[‡]Centre for Molecular and Macromolecular Studies, Polish Academy of Sciences, Lodz, Poland

The ordered arrangement of nanoparticles in one, two and three-dimensional structures is a problem of current interest. While assembly of nanoparticles from solution into monolayer and superlattice structures on solid surfaces has met with a fair degree of success, the controlled assembly of nanoparticles in solution remains a more difficult and relatively unexplored area. In this communication, we describe the assembly of gold nanoparticles in solution using phosphorothioate DNA as a structural interconnect. Sulphur-substituted DNA cross-links the gold nanoparticles in solution through thiolate linkages with the nanoparticle surface, and organizes them in different geometries. The small length of the phosphorothioate DNA molecules used in the study (ca. 4 nm) renders them rigid and effective as connectors between nanoparticles. The organization of gold nanoparticles by sulphur-substituted DNA has been followed with UV-vis spectroscopy, Fourier transform infrared spectroscopy and transmission electron microscopy measurements.

AN important challenge in nanotechnology is to tailor the optical, electronic and electrical properties of nanoparticles by controlling their size and shape[1]. The properties of nanomaterials also depend on the ordered arrangement of nanoparticles in predefined geometries, such as linear, two and three-dimensional superstructures[2,3]. These ordered nanoparticle assemblies have tremendous applications as nanowires in the IC chip industry[4], as nanowaveguides for electromagnetic radiation[5] and as photonic material[6]. Attempts have been made to assemble nanoparticles in different geometries by techniques based on solvent evaporation of hydrophobic nanoparticles[7–9], molecular cross-linking in colloidal aggregates[10–12] and template-directed assembly using biomacromolecules such as DNA[2,13], proteins[14] and bacterial S-layers[15].

Among these methods, template-directed assembly of nanoparticles using biomacromolecules such as DNA is of great interest. DNA is an excellent template for nanoassembly because of its physicochemical stability, linearity of the molecular structure and mechanical rigidity[16]. Furthermore, variation in the sequence of bases in synthetic DNA may be used to obtain different geometries such as junctions (forks), polygons and polyhedra[17]. Mirkin and co-workers[18,19] have shown that DNA is an excellent template for programming the assembly of nanoscale structures into periodic two and three-dimensional structures, and that this approach may be utilized to develop a colorimetric detection scheme for DNA[18,19]. In other reports, Alivisatos and co-workers[20] have shown how gold nanoparticles can be arranged on a single oligonucleotide template. In all these approaches, gold nanoparticles are capped with 3′ or 5′-thiolated, single-stranded DNA sequences which are complimentary to each other and Watson–Crick base-pairing is used to control the relative spatial arrangement of nanoparticles in the hybridized superstructures. One limitation of this approach is that the duplex DNA is not sufficiently rigid to dictate a precise spatial arrangement of nanoparticles.

In this communication, we demonstrate that phosphorothioate DNA [sulphur-substituted DNA (S-DNA), Chart 1] may be used as efficient agents for cross-linking gold nanoparticles in a rigid superstructure. Simple addition of sulphur-substituted DNA to a gold hydrosol results in binding of the nanoparticles to the DNA via sulphur atoms in the DNA backbone and their cross-linking in solution. The use of small phosphorothioate DNA molecules (~ 40 Å long) renders them rigid and applicable as versatile connectors between the gold nanoparticles. To the best of our knowledge, the use of sulphur-substituted DNA as nanoparticle assemblers has not been demonstrated so far. Presented below are details of the investigation.

Gold colloidal particles were prepared by borohydride reduction of aqueous $HAuCl_4$ solution as described elsewhere[21]. This resulted in a clear ruby-red gold solution at pH 9 bearing particles of size 35 ± 7 Å (ref. 21). The pH of the colloidal gold solution was adjusted to 7 using dilute HCl. All UV-vis spectroscopy measurements were carried out on a Hewlett–Packard HP 8542A diode array

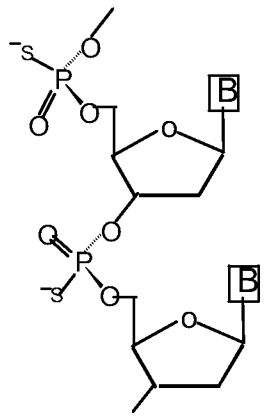

Chart 1.

#For correspondence. (e-mail: sastry@ems.ncl.res.in)

spectrophotometer operated at a resolution of 2 nm. After formation of the colloidal gold solution, S-DNA was added to the solution to yield an overall DNA concentration of 10^{-7} M in the gold–DNA mixture. The sulphur-substituted oligonucleotides were synthesized as described elsewhere[22,23]. The base sequence and length of S-DNA were TTTTTTTTTTTT and roughly 40 Å respectively. The S-DNA–nanogold solution was kept for 2 h to enable the assembly of the gold particles to reach completion, following which drop-coated films of the S-DNA–nanogold complexes were formed on Si (111) substrates and carbon-coated copper grids for Fourier transform infrared (FTIR) spectroscopy and transmission electron microscopy (TEM) measurements respectively. FTIR measurements were carried out in the diffuse reflectance mode on a Shimadzu 8201 PC instrument operated at a resolution of 4 cm^{-1}. TEM measurements were performed on a JEOL Model 1200EX instrument operated at an accelerating voltage of 120 kV.

The gold nanoparticle–S-DNA solution at various stages of preparation was subjected to UV-vis spectroscopy measurements and the spectra obtained are shown in Figure 1 *a*. Curves 1, 2 and 3 correspond to spectra recorded from the gold colloidal solution (before addition of S-DNA), S-DNA–gold nanoparticle solution and pure aqueous S-DNA solution respectively. The spectrum of the colloidal gold solution before addition of S-DNA shows a sharp resonance at 516 nm (curve 1) which broadens and shifts to the red upon complexation with S-DNA molecules (curve 2). The absorption band at 516 nm arises due to excitation of surface plasmon vibrations in the gold nanoparticles and is responsible for their lovely ruby-red colour[18,21]. The red-shift in the surface plasmon resonance band clearly indicates surface co-ordination of the S-DNA molecules with the gold nanoparticles, while the broadening of this absorption band suggests cross-linking of the gold nanoparticles in solution[3,18]. We would like to mention that DNA solution is colourless and does not show any absorption in the visible region of the electromagnetic spectrum (curve 3).

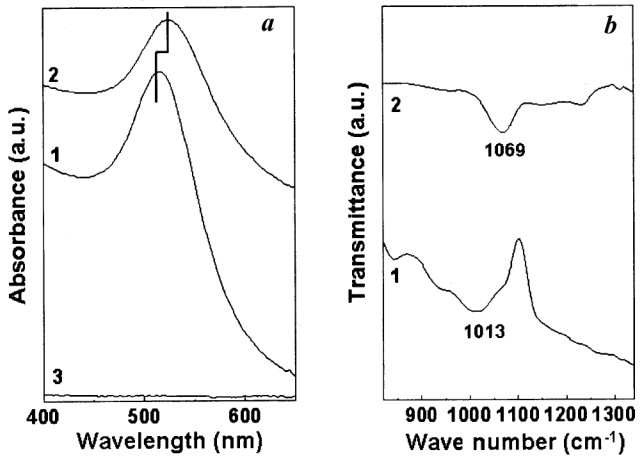

Figure 1. ***a***, UV-vis spectra of the borohydride-reduced, gold colloidal solution (curve 1) and gold solution after addition of S-DNA and aging for 2 h (curve 2). Curve 3 represents the spectrum recorded from pure aqueous S-DNA solution (see text for details). ***b***, FTIR spectra of drop-coated films of pure S-DNA (curve 1) and S-DNA–gold nanoparticle complexes (curve 2) on Si (111) substrate.

Figure 1 *b* shows the FTIR spectra recorded from drop-coated films of pure S-DNA (curve 1) and S-DNA–gold nanoparticle complexes (curve 2) on Si (111) wafers. The S-DNA film exhibits an absorption band centred at 1013 cm^{-1}, this band corresponding to the P-S^- stretching vibration (curve 1). This band is broad and may be due to resonance between S and O atoms in the phosphate backbone. On complexation of S-DNA with the gold nanoparticles, this band becomes sharper and shifts to 1069 cm^{-1}. This clearly indicates that S-DNA molecules bind to gold nanoparticles through the sulphur atoms, as illustrated in Scheme 1.

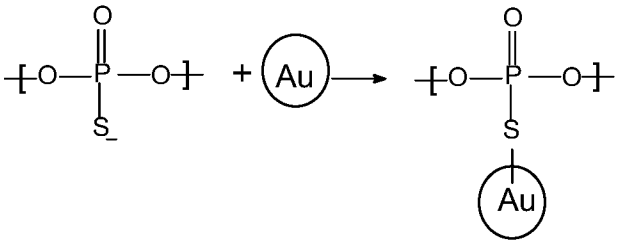

Scheme 1.

Figure 2 *a* and *b* shows representative TEM pictures recorded from films of S-DNA–Au nanoparticle complexes prepared by drop-coating the 2-h-old solution on a TEM grid. For comparison, the TEM micrograph obtained from a drop-coated film of gold nanoparticles before complexation with S-DNA molecules is shown in Figure 2 *c*. From a comparison of Figure 2 *a* and *b* with *c*, it is clear that the particles assemble into loose, open structures consequent to complexation with S-DNA. In the case of the parent gold nanoparticle solution (i.e. without S-DNA), the particles assemble into a dense, close-packed structure after evaporation of water (Figure 2 *c*). This distinguishing feature indicates that the S-DNA molecules bound to the surface of gold nanoparticles prevent their rapid assembly and hold them in place in quasi-linear, open structures. In some regions, fairly long and linear arrangement of nanoparticles is observed (Figure 2 *a*). Another important observation is the difference in separation between the gold nanoparticles after (Figure 2 *a* and *b*) and before complexation with S-DNA molecules (Figure 2 *c*). The separation between the particles is larger (and more uniform) in the case of the S-DNA–Au nanoparticle sample (Figure 2 *a* and *b*) than that observed for gold nanoparticles before complexation with S-DNA (Figure 2 *c*). Figure 3 *a* and *b* shows histograms of the gold nanoparticle edge–edge distances measured from the

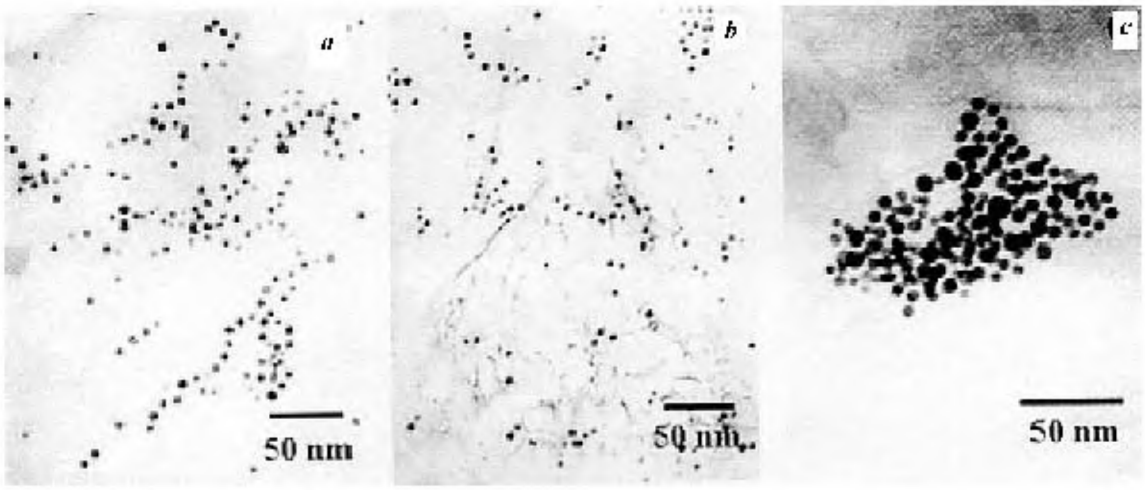

Figure 2. *a* and *b*, Representative TEM pictures of drop-coated films of gold-S-DNA complexes on carbon-coated grids; *c*, TEM picture of drop-coated film of borohydride-reduced gold nanoparticles before complexation with S-DNA on a carbon-coated TEM grid.

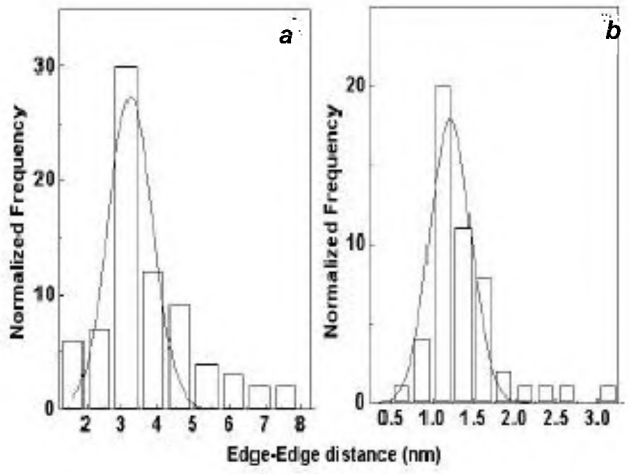

Figure 3. Histogram of edge–edge distances between gold nanoparticles (*a*) cross-linked with S-DNA molecules and (*b*) before complexation with S-DNA. Solid curves in both figures represent Gaussian fits to the histograms.

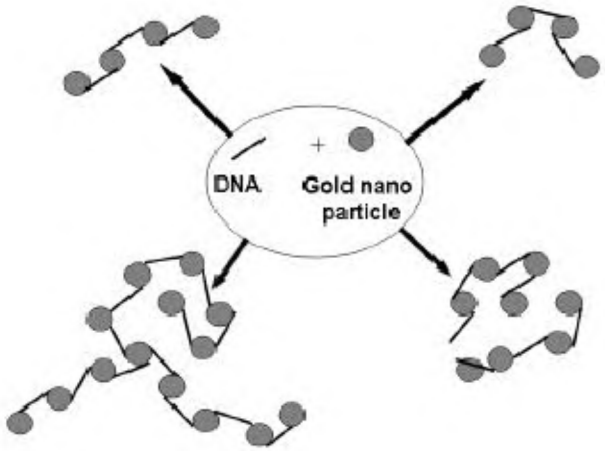

Figure 4. Schematic of possible gold nanoparticle superstructures formed in solution using S-DNA interconnects.

TEM micrographs of Figure 2 for the S-DNA–Au nanoparticle and starting gold nanoparticle samples respectively. A Gaussian fit to the histograms yielded an edge–edge distance for S-DNA–Au nanoparticle complexes and gold nanoparticles before complexation with DNA of 32 ± 6 Å and 12 ± 2 Å respectively. The edge–edge separation between gold nanoparticles complexed with S-DNA is in good agreement with the length of S-DNA molecule of ~ 40 Å. We believe that the presence of a well-defined peak at 32 Å in the interparticle edge–edge distance histogram is a clear indication that the S-DNA molecules bind to the gold nanoparticles only through terminal sulphur atoms in the DNA, as depicted in Figure 4. On the length scale of 40 Å, S-DNA acts like a rigid linker between the gold nanoparticles and the superstructures observed in Figure 2 *a* and *b* may be easily constructed from the connector, as illustrated in Figure 4. Unlike in the case of other DNA-based gold nanoparticle cross-linking strategies that rely on hybridization of complementary DNA molecules for superstructure formation, S-DNA *covalently cross-links the gold nanoparticles* and will conceivably lead to greater stability and possible electronic conduction between the nanoparticles via the covalently linked DNA backbone. Future efforts will be aimed at altering the length of the S-DNA interconnect, obtaining structurally more complex geometries of the DNA linkers and studying the electrical transport properties of the nanoparticle superstructures.

1. Jin, R., Cao, Y.-W. C., Mirkin, C. A., Kelly, K. L., Schatz, G. C. and, Zheng, J. G., *Science*, 2000, **294**, 1901–1903.
2. Kumar, A., Pattarkine, M., Bhadbhade, M., Mandale, A. B., Ganesh, K. N., Dater, S. S., Dharmadhikari, C. V. and Sastry, M., *Adv. Mater.*, 2001, **13**, 341–344.
3. Storhoff, J. J., Lazarides, A. A., Mucic, R. C., Mirkin, C. A., Letsinger, R. L. and Schatz, G. C., *J. Am. Chem. Soc.*, 2000, **122**, 4640–4650.

4. Miao, Z., Xu, D., Ouyang, J., Guo, G., Zhao, X. and Tang, Y., *Nano Lett.*, 2002, **2**, 717–720.
5. Maier, S. A., Brongersma, M. L., Kik, P. G., Meltzer, S., Requicha, A. A. G. and Atwater, H. A., *Adv. Mater*, 2001, **13**, 1501–1505.
6. Kumarswamy, G., Dibaj, A. M. and Caruso, F., *Langmuir*, 2002, **18**, 4150–4154.
7. Petit, C., Taleb, A. and Pileni, M-P., *Adv. Mater.*, 1998, **10**, 259–261.
8. Murray, C. B., Kagan, C. R. and Bawendi, M. G., *Science*, 1995, **270**, 1335–1338.
9. Vossmeyer, T., Reck, G., Katsikas, L., Haupt, E. K. T., Schulz, B. and Weller, H., *ibid*, 1995, **267**, 1476–1479.
10. Korgel, B. A. and Fitzmaurice, D., *Adv. Mater.*, 1998, **10**, 661–665.
11. Andres, R. P. *et al.*, *Science*, 1996, **273**, 1690–1693.
12. Fink, J., Kiely, C. J., Bethell, D. and Schiffirin, D. J., *Chem. Mater.*, 1998, **10**, 922–926.
13. Niemeyer, C. M., Burger, W. and Peplies, J., *Angew. Chem., Int. Ed. Engl.*, 1998, **37**, 2265–2268.
14. Li, M., Wong, Kim, K. W. and Mann, S., *Chem. Mater.*, 1999, **11**, 23–26.
15. Shenton, W., Pum, D., Sleytr, U. B. and Mann, S., *Nature*, 1997, **389**, 585–587.
16. Saenger, W., *Principles of Nucleic Acid Structure*, Springer-Verlag, Berlin, 1987.
17. Seeman, N. C., *Nano. Lett.*, 2001, **1**, 22–26.
18. Mirkin, C. A., Letsinger, R. L., Mucic, R. C. and Storhoff, J. J., *Nature*, 1996, **382**, 607–609.
19. Cao, Y. W., Jin, R. and Mirkin, C. A., *J. Am. Chem. Soc.*, 2001, **123**, 7961–7962.
20. Alivisatos, A. P., Johnsson, K. P., Peng, X. G., Wilson, T. E., Loweth, C. J., Bruchez, M. P. and Schultz, P. G., *Nature*, 1996, **382**, 609–611.
21. Patil, V., Malvankar, R. B. and Sastry, M., *Langmuir*, 1999, **15**, 8197–8206.
22. Ravikumar, V. T. and Cheruvallath, Z. S., *Nucleosides Nucleotides*, 1996, **15**, 1149–1155.
23. Battistini, C., Brasca, M. G., Fustinoni, S. and Lazzari, E., *Tetrahedron*, 1992, **48**, 3209–3226.

ACKNOWLEDGEMENTS. A.K. and S.P. thank the Council of Scientific and Industrial Research (CSIR), Govt of India and Indo-French Centre for Promotion of Advanced Research, New Delhi for financial assistance.

Received 14 November 2002; revised accepted 4 December 2002

Effect of curcumin analogues on oxidation of haemoglobin and lysis of erythrocytes

P. Venkatesan[†,*], M. K. Unnikrishnan[#], M. Sudheer Kumar[#] and M. N. A. Rao[†]

[#]College of Pharmaceutical Sciences, Manipal 576 119, India
[†]Divi's Laboratories Ltd, C-26, Industrial Estate, Sanath Nagar, Hyderabad 500 018, India

A number of ring-substituted analogues of curcumin were studied for their ability to prevent nitrite-induced oxidation of haemoglobin and lysis of erythrocytes. Phenolic analogues were more active than their non-phenolic counterparts. Many of the active compounds were more potent than standard antioxidants such as tocopherol and trolox. Tetrahydrocurcumin showed higher activity than curcumin, suggesting that unsaturation in the central portion of curcumin may not be important for activity.

CURCUMINS from *Curcuma longa* (turmeric) are potent antioxidants[1,2] and possess a number of therapeutic properties[3]. Many of the biological activities of curcumin are attributed to its antioxidant properties[4–6]. While both phenolic groups and the 1,3-diketone system of curcumin are ascribed for its activity by some reports[7,8], several others suggest that the phenolic group may not be essential[8,9]. In our earlier work[10] to understand the importance of the phenolic group and other substituents in the aromatic ring, several analogues of curcumin were synthesized and studied for their antioxidant activity in models such as inhibition of lipid peroxidation and scavenging of radicals such as 1,1′-diphenyl picryl hydrazyl (DPPH) and 2,2′-azinobis(3-ethyl-benthiazoline-6-sulphonic acid) ($ABTS^{+}$). It was observed that the phenolic group is important and ortho substitution with groups such as methoxy, methyl group enhances the activity. It was also observed that the unsaturation in the side chain was not essential for the activity.

Nitrite is an environmental pollutant causing harm to marine fauna, chiefly by oxidizing the haemoglobin to methaemoglobin. Nitrite (NO_2^-) is formed when *Nitrosomonas* sp. bacteria oxidize ammonia produced by fish and decomposing organic matter[11]. Prolonged exposure to low levels can lead to stress and is often associated with stress-related disease such as bacterial ulcers and fin-rot. At higher levels, it is actively transported across the gills and into the bloodstream of the fish where it oxidizes normal haemoglobin to methaemoglobin that cannot transport oxygen. This results in tissue hypoxia even in the presence of oxygen (functional hypoxia)[12].

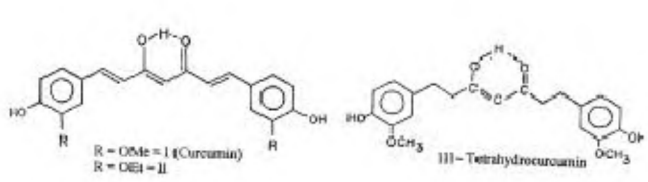

Structure of curcumin and its analogues.

*For correspondence. (e-mail: pvenkat2373@yahoo.com)